International Journal of Mass Spectrometry xxx (2012) xxx–xxx

Contents lists available at SciVerse ScienceDirect

International Journal of Mass Spectrometry

journal homepage: www.elsevier.com/locate/ijms

Competition between diketopiperazine and oxazolone formation in water loss products from protonated ArgGly and GlyArg

Shen Zou[a], Jos Oomens[b,c], Nick C. Polfer[a,*]

[a] Department of Chemistry, University of Florida, P.O. Box 117200, Gainesville, FL 32611, USA
[b] FOM institute for Plasma Physics Rijnhuizen, Edisonbaan 14, 3439 MN Nieuwegein, The Netherlands
[c] University of Amsterdam, Science Park 904, 1098 XH Amsterdam, The Netherlands

ARTICLE INFO

Article history:
Received 24 October 2011
Received in revised form
22 December 2011
Accepted 30 December 2011
Available online xxx

Keywords:
Oxazolone
CID
IR spectroscopy
DFT
Vibrational spectra
Ion spectroscopy

ABSTRACT

The mechanism of peptide "b" fragment formation in collision-induced dissociation (CID) is generally understood as a nucleophilic attack from a carbonyl oxygen onto the electron deficient carbon of the dissociating amide bond forming a five-membered oxazolone ring structure. Nonetheless, other nucleophiles, such as the N-terminus and side-chain moieties (e.g., imidazole, guanidine), can in principle engage in a nucleophilic attack to induce amide backbone cleavage. Here, we apply a combination of infrared multiple photon dissociation (IRMPD) spectroscopy and computational chemistry to characterize the water loss, $[M+H-H_2O]^+$, product ions from protonated ArgGly and GlyArg. IRMPD spectra for $[M+H-H_2O]^+$ from ArgGly and GlyArg differ in the presence and absence of a characteristic band at 1885 cm^{-1}, which is indicative of an oxazolone structure for ArgGly. The remaining parts of the vibrational spectra are consistent with the vibrational signatures of diketopiperazine structures. Conversely, there is no match between the experimental spectra and any of the putative structures arising from guanidine side-chain attack. These results show that the presence of a basic residue, such as arginine, facilitates the formation of diketopiperazine structures, and that residue order matters in the competition between diketopiperazine and oxazolone pathways.

1. Introduction

The formation pathways and structures of peptide *b* ions have been the subject of an on-going debate since the late 1980s. Biemann initially put forward the acylium ion structure [1], but later studies revealed that this structure is unstable and would spontaneously lose CO to become an *a* ion [2–4]. Harrison proposed oxazolone structures for *b* ions, where the C-terminal part of the molecule is stabilized by a 5-membered oxazolone ring [2,3]. As this structure necessitates a nucleophilic attack from a backbone carbonyl, the smallest *b* ions that are typically observed are b_2 fragments, composed of two amino acid residues. An alternative chemical structure for b_2 products is the 6-membered ring diketopiperazine structure, first proposed by Wesdemiotis [5], which involves a nucleophilic attack from the N-terminus. Moreover, nucleophilic attacks from side-chain groups have been suggested in a number of studies. Wysocki and co-workers proposed that enhanced cleavage at His residues is mediated by side chain attack on the backbone carbonyl [6]. O'Hair and co-workers calculated the stability of this 5–5 ring bicyclic structure for the N-acetylated methyl ester of His and found that this structure is more stable than the corresponding protonated oxazolone [7].

In addition to having many possible structures, peptide *b* ions have also been linked with sequence permutation processes in CID [8–18]. A more thorough understanding of peptide fragmentation pathways [19] is hence essential to improve automated interpretation of tandem mass spectra in proteomics. A range of experimental techniques have been applied to confirm structures of *b* ions, including gas-phase hydrogen deuterium exchange (HDX) [13–15,20–25], ion mobility mass spectrometry [26,27], isotope labeling [13,26,28–30], and infrared multiple photon dissociation (IRMPD) spectroscopy [31–34]. Computational methods are essential to support the experimental conclusions, and establish mechanistic pathways [35–38]. Among the structural techniques that have been implemented to confirm the structures of CID product ions, IRMPD spectroscopy is particularly well suited for structural analysis of peptide fragment products [39], as the vibrational spectra can be directly compared to computed linear absorption spectra of putative structures [13,15,39,40].

A statistical analysis of CID mass spectra from tryptic peptides by Zubarev and co-workers showed a considerable preference for b_2 ion formation [41], as opposed to larger *b* ions. A number of studies have suggested that b_2 ions favor an oxazolone structure [42–48]. IRMPD spectroscopy has been used to determine the b_2

* Corresponding author. Tel.: +1 352 392 0492; fax: +1 352 392 0872.
E-mail address: polfer@chem.ufl.edu (N.C. Polfer).

1387-3806/$ – see front matter © 2012 Published by Elsevier B.V.
doi:10.1016/j.ijms.2011.12.020

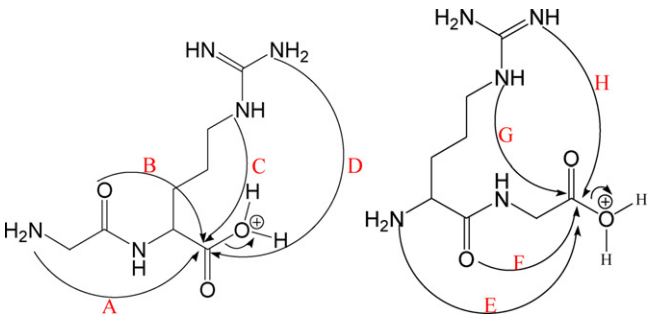

Scheme 1. Water elimination pathways for protonated GlyArg and ArgGly.

ion structure from protonated AGG, AAA, GGG, YGGFL, and tryptic model peptides [13,14,39,40,49–51]. These studies have focused on simple aliphatic residues such as alanine, glycine, or isoleucine, where the side chain is likely to play a more peripheral role in the fragmentation mechanism; the presence of a basic side chain, on the other hand, would be expected to intimately influence the b_2 ion formation pathway and structure. IRMPD results by Wysocki and co-workers on the HA b_2 ion showed evidence for a preponderance of diketopiperazine structures, thus confirming that the presence of the basic histidine residue affects the competition between oxazolone and diketopiperazine formation [22]. Computational modeling of b_2 ions containing arginine and lysine showed that larger cyclic structures formed through side chain reactions are more stable than oxazolone structures [7]. In addition, O'Hair and co-workers compared the fragmentation patterns of histidine-containing b_2 ions from protonated HG-OMe, GH-OMe, HGG-OMe, and GHG-OMe with the GH diketopiperazine and found the fragmentation spectra to be very similar, indicating the formation of a diketopiperazine b_2 ion [52].

In this paper, we applied IRMPD spectroscopy in combination with quantum-chemical computations to characterize the $[M+H-H_2O]^+$ product ions from ArgGly and GlyArg. The presence of the basic guanidine side chain in principle facilitates a number of fragmentation pathways, which are summarized in Scheme 1. Based on previous computational studies [36,38] on water elimination from dipeptides, a charge-directed nucleophilic attack could take place from the N-terminus (A and E), the carbonyl oxygen (B and F), or the side-chain group (C, D, G, and H).

2. Experimental methods

2.1. Sample preparation

The dipeptides ArgGly and GlyArg (Sigma–Aldrich, St. Louis, MO, USA) were employed without further purification and used as 200 μM solution in 50:50 water/methanol with 2% acetic acid to aid protonation.

2.2. Mass spectrometry and infrared multiple photon dissociation spectroscopy

The infrared photodissociation experiments were conducted at the FOM institute for Plasma Physics "Rijnhuizen" using the free electron laser FELIX [53] coupled to a laboratory-built Fourier transform ion cyclotron resonance (FT-ICR) mass spectrometer [54,55]. The $[M+H-H_2O]^+$ CID products were generated by "nozzle-skimmer" dissociation in a commercial Z-spray electrospray ionization (ESI) source (Micromass, Manchester, UK). In order to optimize ion signal on the $[M+H-H_2O]^+$ CID product (i.e., m/z 214), a large DC voltage drop of 160 V was employed between the cone and hexapole. Representative nozzle-skimmer dissociation mass spectra for [GlyArg + H] and [ArgGly + H] are shown in Fig. S1 in the Supplementary Data. These mass spectra show that other CID products are produced abundantly, in particular the ammonia loss product [Arg + H-NH_3]. The fragment ion was accumulated in the hexapole, prior to transfer to the ICR cell. Following mass isolation, the ion of interest was irradiated with the tunable output from the free electron laser. FELIX produces macropulses (5 μs) at a repetition rate of 5 Hz that consist of a train of micropulses at a GHz repetition rate. The pulse energy per macropulse varies as a function of wavelength, reaching maximum values of ~60 mJ at 12 μm. In these experiments, 15 macropulses were employed to induce efficient photodissociation (corresponding to an ion trapping time of 3 s). In the IRMPD process tens to hundreds of photons are absorbed when the laser frequency is in resonance with a fundamental vibration in the molecule, thus leading to photodissociation. This manifests itself in the mass spectrum by a depletion of the precursor ion and appearance of photofragments. The IR photodissociation spectrum was obtained by plotting the IRMPD yield as a function of the wavelength, using the following relation:

$$\text{yield} = -\ln\left[1 - \left(\frac{\sum(\text{photofragments})}{\sum(\text{photofragments} + \text{precursor})}\right)\right]$$

This yield was further normalized with laser power at each wavelength step.

2.3. Computations

A procedure for generating candidate structures for the ArgGly and GlyArg $[M+H-H_2O]^+$ fragments was developed in-house, and has been described previously [13]. The chemical structures (oxazolone, diketopiperazine, and side-chain macrocycles) were built and optimized using semi-empirical approaches (AM1) in Hyperchem (Hypercube Inc., Gainesville, FL), taking into account their preferred sites of proton attachment. While proton attachment at the N-terminus, the guanidine side-chain, the oxazolone ring nitrogen and backbone were all considered, protonation at the guanidine group was significantly favored in all cases. All input structures were optimized using density functional theory (DFT) (B3LYP/6-31 g*) methods in Gaussian03 [56]. The geometry and ESP-derived charges were imported into the AMBER [57] suite of programs, where a restrained electrostatic potential (RESP) [58] fitting was applied. This parameterization procedure was performed for all chemically distinct structures.

For the conformational search, annealing simulation runs with starting temperatures at 300 K and ending at 0 K were carried out, resulting in 300 candidate structures per dynamics simulation. Those structures were then compared with each other using a root-mean-square deviation (RMSD) procedure to remove analogues. All retained output structures from AMBER were then re-optimized at the DFT level, initially using B3LYP/3-21 in Gaussian03. Further optimization was performed both at the B3LYP/6-31g* and finally at the B3LYP/6-31g** levels. The electronic energy for each conformer at the B3LYP/6-31g** level was corrected for the zero-point energy (ZPE) at the same level to yield the final ZPE-corrected energies. All energies are presented here relative to the lowest-energy conformers found for the ArgGly and GlyArg $[M+H-H_2O]^+$ fragments, respectively. The vibrational spectra of the lowest-energy structures at the B3LYP/6-31g** level are scaled by 0.975 in the 1200–2000 cm^{-1} range.

Please cite this article in press as: S. Zou, et al., Int. J. Mass Spectrom. (2012), doi:10.1016/j.ijms.2011.12.020

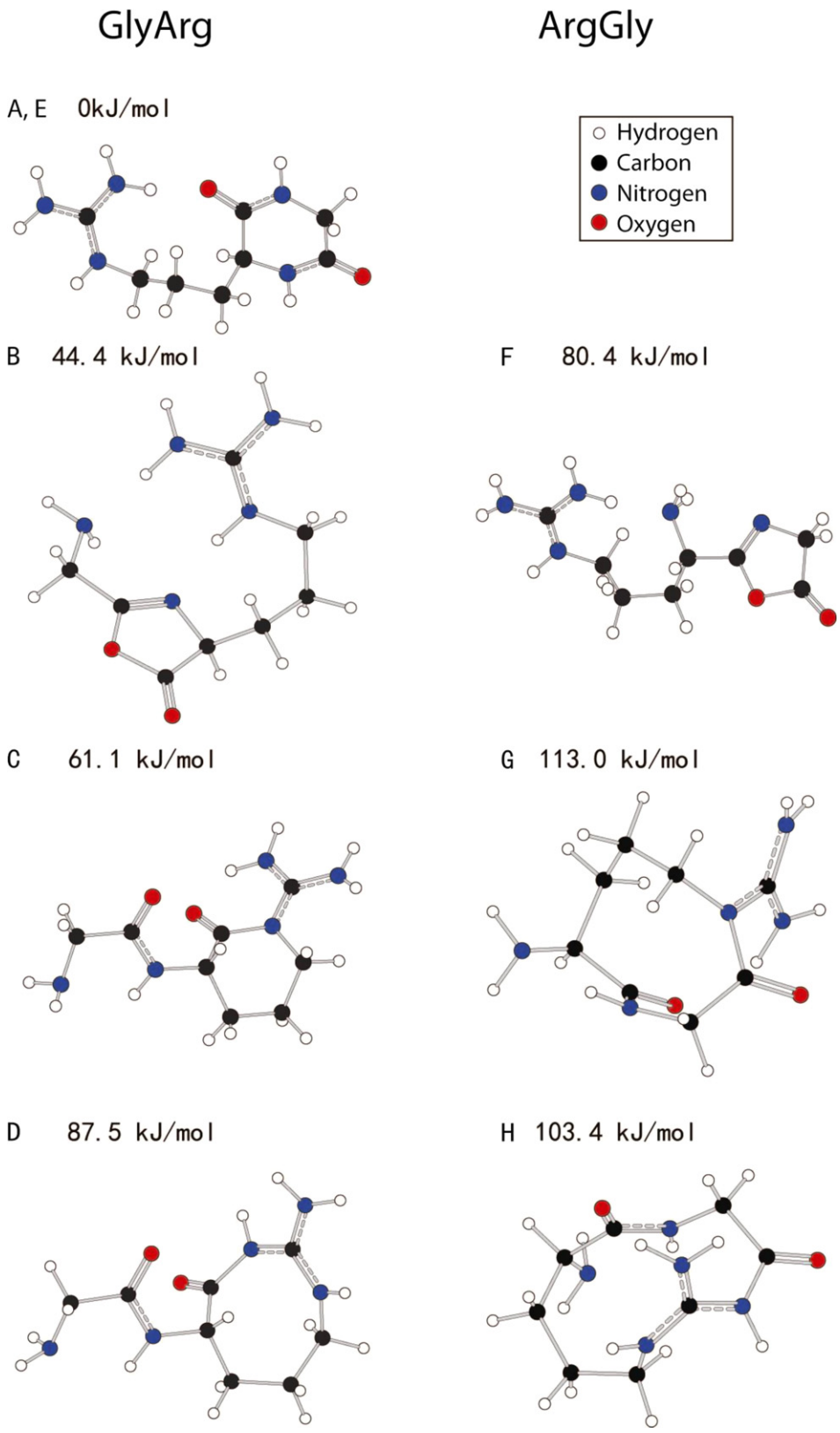

Fig. 1. Calculated geometries and relative energies of the $[M+H-H_2O]^+$ products for ArgGly and GlyArg: diketopiperazine structures protonated on the guanidine N (A and E), oxazolone structures protonated on the guanidine N (B and F), and guanidine side-chain induced structures protonated on the guanidine group (C, D, G, and H).

Please cite this article in press as: S. Zou, et al., Int. J. Mass Spectrom. (2012), doi:10.1016/j.ijms.2011.12.020

Table 1
Electronic, ZPE-corrected and Gibbs free energies at 298 K of the conformers in Fig. 1 computed at the B3LYP/6-31g** level of theory.

	E_{total}/H	E_{total} + ZPE/H	$\Delta(E_{total}$ + ZPE)/ kJ mol^{-1}	ΔG_{298}/kJ mol^{-1}
A and E	−738.569897	−738.303060	0.0	0.0
B	−738.551705	−738.286222	44.4	45.8
C	−738.545636	−738.279760	61.1	60.5
D	−738.536570	−738.269748	87.5	89.0
F	−738.537931	−738.272446	80.4	79.4
G	−738.527135	−738.259879	113.0	121.1
H	−738.531410	−738.263680	103.4	110.8

3. Results and discussion

3.1. Computation results

The lowest-energy conformers for each of the fragmentation pathways in Scheme 1 are presented in Fig. 1. Electronic, ZPE-corrected and Gibbs free energies of these structures are summarized in Table 1. Due to the "head-to-tail" cyclization, the diketopiperazine structure protonated on the guanidine N (A and E) is identical for both GlyArg and ArgGly. The diketopiperazine structure is favored substantially over all other putative geometries, including the oxazolone structures protonated on the guanidine N (B and F), and the guanidine side-chain induced structures protonated on the guanidine group (C, D, G, and H).

3.2. IRMPD results

The IRMPD spectra of the $[M+H-H_2O]^+$ CID products for GlyArg and ArgGly are depicted in Fig. 2. The spectra exhibit many very similar features, with the notable exception of the band at 1885 cm^{-1}, which is only observed in the case of ArgGly.

In Fig. 3, these experimental spectra are compared to the computed linear absorption spectra of the putative structures shown in Fig. 1. Based on this analysis, it is clear that the band at 1885 cm^{-1} can be assigned to the diagnostic oxazolone CO stretch (indicated in light red). The absence of this band in the GlyArg $[M+H-H_2O]^+$ spectrum suggests that the formation of an oxazolone is disfavored in this case. This is surprising at first sight, as the oxazolone structure for GlyArg (Fig. 1B, +44.4 kJ mol^{-1}) is substantially lower in energy than the corresponding structure for ArgGly (Fig. 1F, +80.4 kJ mol^{-1}). The remaining features in the vibrational spectra are nearly identical, showing bands at 1750, 1670, 1400 and 1300 cm^{-1}. These modes closely mirror the calculated vibrational signature of the diketopiperazine structure. While the use of one scaling factor (i.e., 0.975) for all vibrations does not allow an exact matching of all band positions, the general pattern is very similar for both theory and experiment. On the other hand, the side-chain mediated product structures (C, D, G, and H) all predict strong modes in the 1450–1600 and 1800 cm^{-1} range, which are not observed in the experiment. In conclusion, these results confirm a mixture of diketopiperazine and oxazolone for ArgGly, as opposed to the sole presence of diketopiperazine for GlyArg.

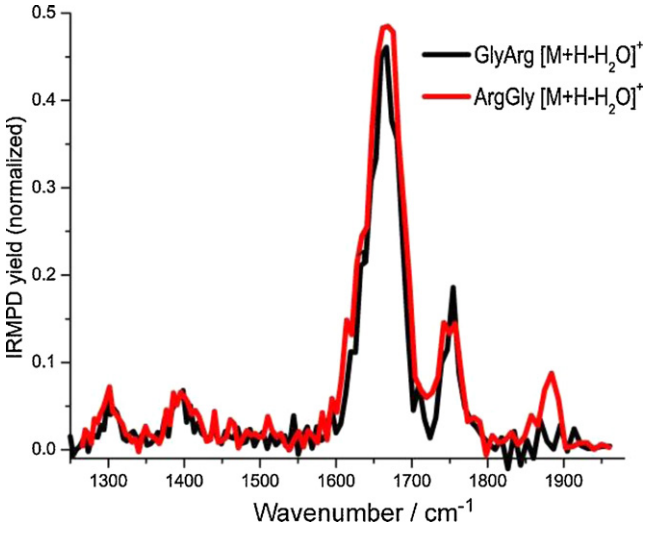

Fig. 2. Experimental IRMPD spectra of $[M+H-H_2O]^+$ from protonated GlyArg and ArgGly.

A comparison of the computed spectra for the ArgGly diketopiperazine and oxazolone structures shows that both structures have diagnostic bands in the mid-IR range. In analogy to the oxazolone-specific band at 1885 cm^{-1}, the diketopiperazine structure exhibits an intense diagnostic band at 1750 cm^{-1}. A rough estimate of the relative abundances of oxazolone vs. diketopiperazine can be made based on the relative experimental band intensities of these diagnostic modes, normalized with the computed integral band intensities for both modes. This suggests a ratio of 57% diketopiperazine vs. 43% oxazolone. Alternatively, a linear combination of the computed IR spectra could be employed to find the best match with the experimental spectrum [59]. A more rigorous approach involves an analysis of the photodissociation kinetics [60].

3.3. Vibrational analysis

An assignment of the IR bands for GlyArg $[M+H-H_2O]^+$ is proposed in Table 2. In contrast, for ArgGly $[M+H-H_2O]^+$, the mixture of structures does not allow an unambiguous identification of all bands, due to some spectral congestion. The intense diketopiperazine-specific band at 1750 cm^{-1} is thus assigned to the unprotonated Gly residue amide I (i.e., CO stretching) mode.

3.4. Mechanistic implications

It is clear from these results that the basic arginine side chain plays a key role in favoring the diketopiperazine pathway. Wysocki and co-workers first reported this for the b_2 ion from HisAla, hypothesizing that "the basicity of the His side chain allows diketopiperazine formation by serving as a protonation site, allowing the unprotonated nucleophilic N-terminal amine to attack the second carbonyl" [42]. In terms of the pathways in competition model [19], the diketopiperazine pathway is typically entropically disfavored, due to the trans–cis isomerization that is required for the former mechanism. Based on the "mobile proton" model [61], the proton is more strongly sequestered on the arginine side chain, thus leading to an increase in the dissociation threshold of the molecule. These trends are hence expected to make the diketopiperazine pathway more competitive in peptides containing basic residues. Intriguingly, for larger *b* fragments the presence of arginine may in fact disfavor "head-to-tail" cyclization, as shown by Van Stipdonk and co-workers [62].

Table 2
Proposed assignment of IR bands for GlyArg $[M+H-H_2O]^+$.

Band position/cm^{-1}	Mode description
1750	Gly amide I mode
1670	Simultaneous Arg amide I mode and deformation modes of the protonated guanidine group
1400	—C—H bending
1300	C—N stretch

Please cite this article in press as: S. Zou, et al., Int. J. Mass Spectrom. (2012), doi:10.1016/j.ijms.2011.12.020

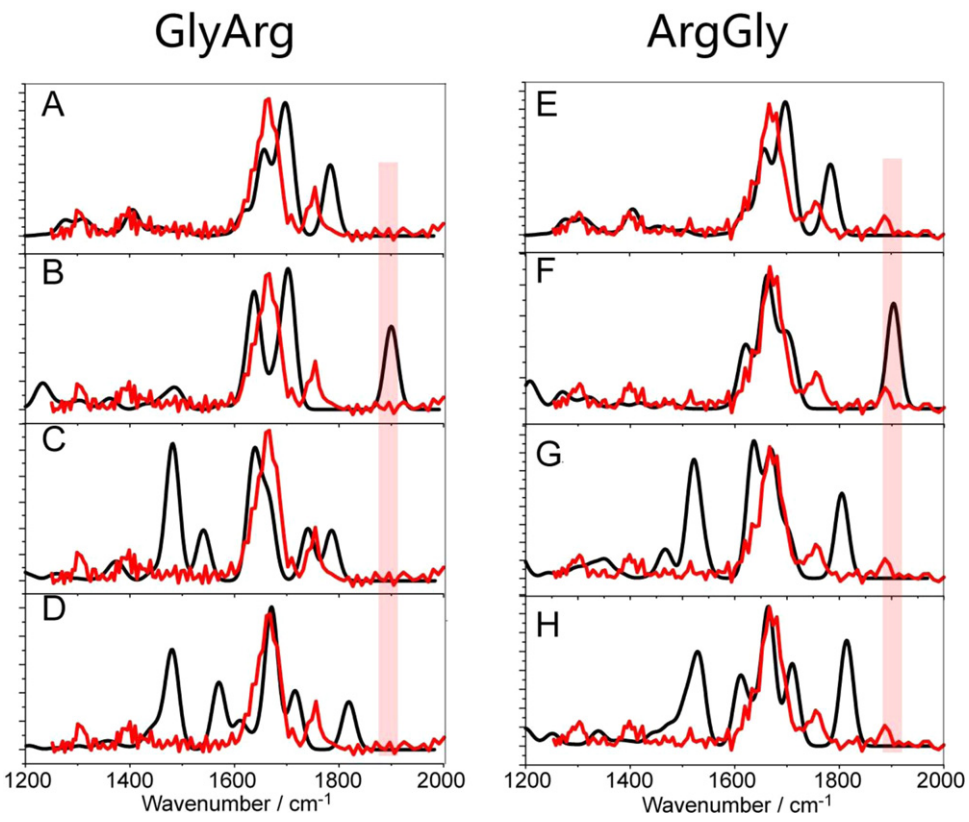

Fig. 3. Experimental IRMPD spectra (red) of the $[M+H-H_2O]^+$products for GlyArg and ArgGly compared to computed linear absorption spectra (black) for the structures shown in Fig. 1: diketopiperazine structures protonated on the guanidine N (A and E), oxazolone structures protonated on the guanidine N (B and F), and guanidine side-chain induced structures protonated on the guanidine group (C, D, G, and H).

Our results further show that the location of the arginine residue affects the competition between diketopiperazine and oxazolone formation. While a detailed modeling of the fragmentation pathways for ArgGly and GlyArg is complicated by the highly flexible arginine side chain, some intuitive understanding may be forthcoming from this observation. In order to adopt the reactive conformation for nucleophilic attack at the carbonyl site, the proton needs to be moved to the C-terminal OH. Given the high basicity of the guanidine group, however, it is conceivable that the proton has an affinity to be shared between the guanidine and the C-terminal OH groups. In an ArgGly configuration, this would result in a more locked conformation, consequently disfavoring a head-to-tail attack from the N-terminus. Conversely, in a GlyArg configuration, the N-terminus would be free to attack the carbonyl site. The subtle differences in energetics from these interactions may explain a slight disfavoring of the diketopiperazine pathway for ArgGly, leading to an opening of the oxazolone pathway.

4. Conclusions

In this paper, IRMPD spectroscopy and computational methods were employed to investigate the effect of the basic amino acid residue arginine, and its order in the peptide sequence, on water elimination fragment products in CID. The vibrational spectra for $[M+H-H_2O]^+$ from protonated GlyArg and ArgGly differ in the presence and absence of a characteristic band at 1885 cm^{-1}, thus confirming an oxazolone structure for ArgGly. Most of the other features in the vibrational spectra are almost identical (1750 cm^{-1}, 1670 cm^{-1}, 1400 cm^{-1} and 1300 cm^{-1}), and are consistent with the presence of a diketopiperazine structure. On the other hand, there is no match between the experimental spectra and any of the structures arising from side-chain attacks. These results confirm that oxazolone structures are not always formed for b_2 ions as previously shown by Perkins et al. [22], particularly if a basic residue is present. Arginine, as the most basic residue, confirms this trend, even if the location of arginine does affect the competition between diketopiperazine and oxazolone formation.

Acknowledgements

The authors would like to thank the FELIX staff for skillful assistance, in particular Dr. Britta Redlich and Dr. Lex van der Meer. Josipa Grzetic is thanked for helping with collection of mass spectra. The UF HPC Center is acknowledged for providing computational resources and support. N.P. thanks the University of Florida for start-up funds and travel support from NSF-PIRE (OISE-0730072). This work is supported by the National Science Foundation under CHE-0845450. Finally, we acknowledge Professor Alex Harrison for his many stimulating contributions to the mass spectrometry community, and peptide fragmentation chemistry in particular.

Appendix A. Supplementary data

Supplementary data associated with this article can be found, in the online version, at doi:10.1016/j.ijms.2011.12.020.

References

[1] K. Biemann, Biomed. Environ. Mass Spectrom. 16 (1988) 99.
[2] T. Yalcin, C. Khouw, I.G. Csizmadia, M.R. Peterson, A.G. Harrison, J. Am. Soc. Mass Spectrom. 6 (1995) 1165.
[3] T. Yalcin, I.G. Csizmadia, M.B. Peterson, A.G. Harrison, J. Am. Soc. Mass Spectrom. 7 (1996) 233.
[4] B. Paizs, Z. Szlavik, G. Lendvay, K. Vekey, S. Suhai, Rapid Commun. Mass Spectrom. 14 (2000) 746.
[5] M. Cordero, J. Houser, C. Wesdemiotis, Anal. Chem. 65 (1993) 1594.

[6] V.H. Wysocki, G. Tsaprailis, L.L. Smith, L.A. Breci, J. Mass Spectrom. 35 (2000) 1399.
[7] J. Farrugia, R.A.J. O'Hair, G. Reid, Int. J. Mass Spectrom. 210/211 (2001) 71.
[8] A.G. Harrison, A.B. Young, B. Bleiholder, S. Suhai, B. Paizs, J. Am. Chem. Soc. 128 (2006) 10364.
[9] A.G. Harrison, J. Am. Soc. Mass Spectrom. 19 (2008) 1776.
[10] S. Molesworth, S. Osburn, M.J. van Stipdonk, J. Am. Soc. Mass Spectrom. 20 (2009) 2174.
[11] A. Harrison, J. Am. Soc. Mass Spectrom. 20 (2009) 2248.
[12] U. Erlekam, B. Bythell, D. Scuderi, M.J. Van Stipdonk, B. Paizs, P. Maitre, J. Am. Chem. Soc. 131 (2009) 11503.
[13] X. Chen, L. Yu, J.D. Steill, J. Oomens, N.C. Polfer, J. Am. Chem. Soc. 131 (2009) 18272.
[14] X. Chen, J.D. Steill, J. Oomens, N.C. Polfer, J. Am. Soc. Mass Spectrom. 21 (2010) 1313.
[15] A. Gucinski, Á. Somogyi, J. Chamot-Rooke, V. Wysocki, J. Am. Soc. Mass Spectrom. 21 (2010) 1329.
[16] I.S. Saminathan, X.S. Wang, Y. Guo, O. Krakovska, S. Voisin, A.C. Hopkinson, K.W.M. Siu, J. Am. Soc. Mass Spectrom. 21 (2010) 2085.
[17] L. Yu, Y. Tan, Y. Tsai, D.R. Goodlett, N.C. Polfer, J. Proteome Res. 10 (2011) 2409.
[18] A.A. Goloborodko, M.V. Gorshkov, D.M. Good, R.A. Zubarev, J. Am. Soc. Mass Spectrom. 22 (2011) 1121.
[19] B. Paizs, S. Suhai, Mass Spectrom. Rev. 24 (2005) 508.
[20] B.J. Bythell, A. Somogyi, B. Paizs, J. Am. Soc. Mass Spectrom. 20 (2009) 618.
[21] K.A. Herrmann, K. Kuppannan, V.H. Wysocki, Int. J. Mass Spectrom. 249/250 (2006) 93.
[22] B. Perkins, J. Chamot-Rooke, S. Yoon, A. Gucinski, A. Somogyi, V.H. Wysocki, J. Am. Chem. Soc. 131 (2009) 17528.
[23] A. Fattahi, B. Zekavat, T. Solouki, J. Am. Soc. Mass Spectrom. 21 (2009) 358.
[24] X. Li, Y. Huang, P.B. O'Connor, C. Lin, J. Am. Soc. Mass Spectrom. 22 (2011) 245.
[25] G.E. Reid, R.J. Simpson, R.A.J. O'Hair, Int. J. Mass Spectrom. 191 (1999) 209.
[26] I. Garcia, K. Giles, R.H. Bateman, S.J. Gaskell, J. Am. Soc. Mass Spectrom. 19 (2008) 1781.
[27] N.C. Polfer, B.C. Bohrer, M.D. Plasencia, B. Paizs, D.E. Clemmer, J. Phys. Chem. A 112 (2008) 1286.
[28] Q. Fu, L. Li, J. Mass Spectrom. 41 (2006) 1600.
[29] U.H. Verkerk, J. Zhao, M.J. Van Stipdonk, B.J. Bythell, J. Oomens, A.C. Hopkinson, K.W.M. Siu, J. Phys. Chem. A 115 (2011) 6683.
[30] J. Leng, H. Wang, L. Zhang, J. Zhang, H. Wang, T. Cai, J. Yao, Y. Guo, J. Am. Soc. Mass Spectrom. 22 (2011) 1204.
[31] J. Oomens, B. Sartakov, G. Meijer, G. von Helden, Int. J. Mass Spectrom. 254 (2006) 1.
[32] L. MacAleese, P. Maitre, Mass Spectrom. Rev. 26 (2007) 583.
[33] T.D. Fridgen, Mass Spectrom. Rev. 28 (2009) 586.
[34] N.C. Polfer, Chem. Soc. Rev. 40 (2011) 2211.
[35] B. Bythell, A. Somogyi, B. Paizs, J. Am. Soc. Mass Spectrom. 20 (2009) 618.
[36] B. Bythell, R. Dain, S. Curtice, J. Oomens, J.D. Steill, G.S. Groenewold, B. Paizs, M.J. Van Stipdonk, J. Phys. Chem. A 114 (2010) 5076.
[37] B. Balta, V. Aviyente, C. Lifshitz, J. Am. Soc. Mass Spectrom. 14 (2003) 1192.
[38] P.B. Armentrout, A.L. Heaton, J. Am. Soc. Mass Spectrom. 8 (2011) 1.
[39] R.K. Sinha, U. Erlekam, B.J. Bythell, B. Paizs, P. Maître, J. Am. Soc. Mass Spectrom. 22 (2011) 1645.
[40] J. Oomens, S. Young, S. Molesworth, M.J. van Stipdonk, J. Am. Soc. Mass Spectrom. 20 (2009) 334.
[41] M.M. Savitski, M. Fälth, Y.M.E. Fung, C.M. Adams, R.A. Zubarev, J. Am. Soc. Mass Spectrom. 19 (2008) 1755.
[42] K. Eckart, M.C. Holthausen, W. Koch, J. Spiess, J. Am. Soc. Mass Spectrom. 9 (1998) 1002.
[43] A.G. Harrison, I.G. Csizmadia, T.-H. Tang, J. Am. Soc. Mass Spectrom. 11 (2000) 427.
[44] B. Paizs, S. Suhai, Rapid Commun. Mass Spectrom. 16 (2002) 375.
[45] B. Paizs, S. Suhai, A.G. Harrison, J. Am. Soc. Mass Spectrom. 14 (2003) 1454.
[46] H. El Aribi, C.F. Rodriquez, D.R.P. Almeida, Y. Ling, W.W.-N. Mak, A.C. Hopkinson, K.W.M. Siu, J. Am. Chem. Soc. 125 (2003) 9229.
[47] H. El Aribi, G. Orlova, A.C. Hopkinson, K.W.M. Siu, J. Phys. Chem. A 108 (2004) 3844.
[48] B.J. Bythell, D.F. Barofsky, F. Pingitore, M.J. Polce, P. Wang, C. Wesdemiotis, B. Paizs, J. Am. Soc. Mass Spectrom. 18 (2007) 1291.
[49] S. Yoon, J. Chamot-Rooke, B. Perkins, A. Hilderbrand, J.C. Poutsma, V.H. Wysocki, J. Am. Chem. Soc. 130 (2008) 17644.
[50] B. Bythell, U. Erlekam, B. Paizs, P. Maitre, Chem. Phys. Chem. 10 (2009) 883.
[51] D. Wang, K. Gulyuz, C.N. Stedwell, N.C. Polfer, J. Am. Soc. Mass Spectrom. 22 (2011) 1197.
[52] J.M. Farrugia, T. Taverner, R.A.J. O'Hair, Int. J. Mass Spectrom. 209 (2001) 99.
[53] D. Oepts, A.F.G. van der Meer, P.W. van Amersfoort, Infrared Phys. Technol. 36 (1995) 297.
[54] N.C. Polfer, J. Oomens, D.T. Moore, G. von Helden, G. Meijer, R.C. Dunbar, J. Am. Chem. Soc. 128 (2006) 517.
[55] J.J. Valle, J.R. Eyler, J. Oomens, D.T. Moore, A.F.G. van der Meer, G. von Helden, G. Meijer, C.L. Hendrickson, A.G. Marshall, G.T. Blakney, Rev. Sci. Instrum. 76 (2005) 23103.
[56] M.J. Frisch, G.W. Trucks, H.B. Schlegel, G.E. Scuseria, M.A. Robb, J.R. Cheeseman, J.A. Montgomery Jr., T. Vreven, K.N. Kudin, J.C. Burant, J.M. Millam, S.S. Iyengar, J. Tomasi, V. Barone, B. Mennucci, M. Cossi, G. Scalmani, N. Rega, G.A. Petersson, H. Nakatsuji, M. Hada, M. Ehara, K. Toyota, R. Fukuda, J. Hasegawa, M. Ishida, T. Nakajima, Y. Honda, O. Kitao, H. Nakai, M. Klene, X. Li, J.E. Knox, H.P. Hratchian, J.B. Cross, V. Bakken, C. Adamo, J. Jaramillo, R. Gomperts, R.E. Stratmann, O. Yazyev, A.J. Austin, R. Cammi, C. Pomelli, J.W. Ochterski, P.Y. Ayala, K. Morokuma, G.A. Voth, P. Salvador, J.J. Dannenberg, V.G. Zakrzewski, S. Dapprich, A.D. Daniels, M.C. Strain, O. Farkas, D.K. Malick, A.D. Rabuck, K. Raghavachari, J.B. Foresman, J.V. Ortiz, Q. Cui, A.G. Baboul, S. Clifford, J. Cioslowski, B.B. Stefanov, G. Liu, A. Liashenko, P. Piskorz, I. Komaromi, R.L. Martin, D.J. Fox, T. Keith, M.A. Al-Laham, C.Y. Peng, A. Nanayakkara, M. Challacombe, P.M.W. Gill, B. Johnson, W. Chen, M.W. Wong, C. Gonzalez, J.A. Pople, Gaussian03, Revision C.02, Gaussian, Inc., Wallingford, CT, 2004.
[57] W.D. Cornell, P. Cieplak, C.I. Bayly, I.R. Gould, K.M. Merz Jr., D.M. Ferguson, D.C. Spellmeyer, T. Fox, J.W. Caldwell, P.A. Kollmann, J. Am. Chem. Soc. 117 (1995) 5179.
[58] P. Cieplak, W.D. Cornell, C.I. Bayly, P.A. Kollmann, Computat. Chem. 16 (1995) 1357.
[59] U. Verkerk, C.-K. Siu, J. Steill, H. El Aribi, J. Zhao, C. Rodriquez, J. Oomens, A. Hopkinson, K. Siu, J. Phys. Chem. Lett. 1 (2010) 868.
[60] J. Prell, T. Chang, G. Biles, G. Berden, J. Oomens, E. Williams, J. Phys. Chem. A 115 (2011) 2745.
[61] A.R. Dongre, J.L. Jones, A. Somogyi, V.H. Wysocki, J. Am. Chem. Soc. 118 (1996) 8365.
[62] S. Molesworth, S. Osburn, M.J. van Stipdonk, J. Am. Soc. Mass Spectrom. 21 (2010) 1028.

Please cite this article in press as: S. Zou, et al., Int. J. Mass Spectrom. (2012), doi:10.1016/j.ijms.2011.12.020